

Gene Knockdown by EpCAM Aptamer-siRNA Chimeras Suppresses Epithelial Breast Cancers and Their Tumor-Initiating Cells

Adi Gilboa-Geffen¹, Peter Hamar^{1,2}, Minh T.N. Le¹, Lee Adam Wheeler¹, Radiana Trifonova¹, Fabio Petrocca¹, Anders Wittrup¹, and Judy Lieberman¹

Abstract

Effective therapeutic strategies for *in vivo* siRNA delivery to knockdown genes in cells outside the liver are needed to harness RNA interference for treating cancer. EpCAM is a tumor-associated antigen highly expressed on common epithelial cancers and their tumor-initiating cells (TIC, also known as cancer stem cells). Here, we show that aptamer-siRNA chimeras (AsiC, an EpCAM aptamer linked to an siRNA sense strand and annealed to the siRNA antisense strand) are selectively taken up and knock down gene expression in EpCAM⁺ cancer cells *in*

vitro and in human cancer biopsy tissues. *PLK1* EpCAM-AsiCs inhibit colony and mammosphere formation (*in vitro* TIC assays) and tumor initiation by EpCAM⁺ luminal and basal-A triple-negative breast cancer (TNBC) cell lines, but not EpCAM⁻ mesenchymal basal-B TNBCs, in nude mice. Subcutaneously administered EpCAM-AsiCs concentrate in EpCAM⁺ Her2⁺ and TNBC tumors and suppress their growth. Thus, EpCAM-AsiCs provide an attractive approach for treating epithelial cancer. *Mol Cancer Ther*; 14(10); 2279–91. ©2015 AACR.

Introduction

RNA interference (RNAi) offers the opportunity to treat disease by knocking down disease-causing genes (1). Recent early-phase clinical trials have shown vigorous (75%–95%), sustained (lasting up to several months) and safe knockdown of a handful of gene targets in the liver using lipid nanoparticle-encapsulated or GalNAc-conjugated siRNAs (2–5). The liver, the body's major filtering organ, traps particles and, hence, is relatively easy to transfect. The major obstacle to harnessing RNAi for treating most diseases, however, has yet to be solved, namely efficient delivery of small RNAs and gene knockdown in cells beyond the liver. In particular, the delivery roadblock is a major obstacle to harnessing RNAi to treat cancer (6).

Triple-negative breast cancer (TNBC), a heterogeneous group of poorly differentiated cancers defined by the lack of estrogen, progesterone, and Her2 receptor expression, has the worst prognosis of any breast cancer subtype (7–9). Most TNBCs have epithelial properties and are classified as basal-like, although a sizable minority are mesenchymal. TNBC afflicts younger women and is the subtype associated with *BRCA1* genetic mutations. No targeted therapy is available. Although most TNBC patients

respond to chemotherapy, within 3 years about a third develop metastases and eventually die. Thus, new approaches are needed.

Here we develop a flexible, targeted platform for gene knockdown and treatment of basal-like TNBCs that might also be suitable for therapy against most of the common (epithelial) cancers. We deliver siRNAs into epithelial cancer cells by linking them to an RNA aptamer that binds to EpCAM, the first described tumor antigen, a cell surface receptor overexpressed on epithelial cancers, including basal-like TNBCs. Aptamer-linked siRNAs, known as aptamer-siRNA chimeras (AsiC), have been used in small animal models to treat prostate cancer and prevent HIV infection (10–18). We chose EpCAM for targeting basal-like TNBC because EpCAM is highly expressed on all epithelial cancers. A high affinity EpCAM aptamer was previously identified (19). EpCAM also marks tumor-initiating cells (TIC, also known as cancer stem cells; refs. 20–27). Although the cancer stem cell hypothesis may not apply to all tumors, most solid cancers are heterogeneous and the less differentiated TIC subpopulation is probably responsible for initiating tumors, resistant to conventional cytotoxic drugs and responsible for recurrence and metastases. Devising therapies to eliminate TICs is an important unmet goal of cancer research (28).

In normal epithelia, EpCAM is only weakly expressed on basolateral gap junctions, where it may not be accessible to drugs (29). In epithelial cancers, it is not only more abundant (by several orders of magnitude), but is also distributed along the cell membrane. Ligation of EpCAM promotes adhesion and enhances cell proliferation and invasivity. Proteolytic cleavage of EpCAM releases an intracellular fragment that increases stem cell factor transcription (30, 31). EpCAM's oncogenic properties may make it difficult for tumor cells to develop resistance by down-modulating EpCAM. In one study, about 2/3 of TNBCs, presumably the basal-like subtype, stained strongly for EpCAM (25). The number of EpCAM⁺ circulating cells is linked to poor prognosis in breast cancer (32–36). An EpCAM antibody has been evaluated

¹Cellular and Molecular Medicine Program, Boston Children's Hospital and Department of Pediatrics, Harvard Medical School, Boston, Massachusetts. ²Institute of Pathophysiology, Semmelweis University, Budapest, Hungary.

Note: Supplementary data for this article are available at Molecular Cancer Therapeutics Online (<http://mct.aacrjournals.org/>).

Corresponding Author: Judy Lieberman, Boston Children's Hospital, Harvard Medical School, 200 Longwood Avenue, Boston, MA 02115. Phone: 617-713-8600; Fax: 617-713-8620; E-mail: judy.lieberman@childrens.harvard.edu

doi: 10.1158/1535-7163.MCT-15-0201-T

©2015 American Association for Cancer Research.

clinically for epithelial cancers, but had limited effectiveness on its own (37–39). EpCAM expression identifies circulating tumor cells in an FDA-approved method for monitoring metastatic breast, colon, and prostate cancer treatment (32–36). Moreover, about 97% of human breast cancers and virtually 100% of other common epithelial cancers, including lung, colon, pancreas, and prostate, stain brightly for EpCAM (23), suggesting that the platform developed here could be adapted for RNAi-based therapy of common solid tumors.

Here we show that epithelial breast cancer cell lines uniformly stain brightly for EpCAM, while immortalized normal breast epithelial cells, fibroblasts, and mesenchymal tumor cell lines do not. EpCAM-AsiCs cause targeted gene knockdown in luminal and basal-A TNBC cancer cell lines (which resemble basal-like TNBC primary tumors), and human breast cancer tissues *in vitro*, but not in normal epithelial cells, basal-B TNBC cell lines (which resemble mesenchymal TNBC primary tumors) or normal human breast tissues. Knockdown is proportional to EpCAM expression. Moreover, EpCAM-AsiC-mediated knockdown of *PLK1*, a gene required for mitosis, suppresses *in vitro* TIC functional assays (colony and mammosphere formation) of epithelial breast cancer lines. *Ex vivo* treatment specifically abrogates tumor initiation. Subcutaneously injected *PLK1* EpCAM-AsiCs are taken up specifically by EpCAM⁺ xenografts of poor prognosis basal-A and Her2 breast cancers and cause rapid tumor regression.

Materials and Methods

Cells

MDA-MB-468 (MB468) cells transduced with a Firefly luciferase reporter (MB468-luc) were kindly provided by Andrew Kung (Columbia University, New York NY). BPE and BPLER cells, provided by Tan Ince (University of Miami, Miami, FL), were maintained in supplemented WIT-T medium (Stemgent). Other human cell lines were obtained from ATCC and grown in MEM (MCF7, BT474), McCoy's 5A (SKBR3), RPMI1640 (HCC1806, HCC1143, HCC1937, HCC1954, HCC1187, MB468, T47D), or DMEM (MB231, BT549, MB436) media supplemented with 10% FBS (Gemini Bioproducts), 100 U/mL penicillin G and 100 µg/mL streptomycin sulfate, 6 mmol/L HEPES, 1.6 mmol/L L-glutamine, 50 µmol/L β-mercaptoethanol (Sigma-Aldrich). MCF10CA1a cells, provided by Karmanos Cancer Institute (Detroit, MI), were grown in supplemented DMEM. MB231 cells stably expressing Firefly luciferase and mCherry (MB231-luc-mCherry) were selected after infection with pLV-Fluc-mCherry-Puro lentivirus (provided by Andrew Kung) using puromycin. The authors have not authenticated the cell lines used. Cell lines were obtained in 2012 and were expanded briefly before aliquoting and freezing. Cells used for experiments were thawed from low passage aliquots. All cell lines were verified to be free of mycoplasma.

RNAs

The long strand of the AsiC synthesized with 2'-fluoropyrimidines (TriLink Biotechnologies) was annealed to the short antisense strand (Integrated DNA Technologies) using a 2-fold molar excess of the short strand. The long strand was heated to 95°C for 10 minutes before adding the short strand that was annealed at 65°C for 7 minutes. The mixture was allowed to cool at room temperature for 20 minutes. The annealed AsiC duplexes were purified further using Illustra MicroSpin G-25 columns (GE

Healthcare Life Sciences). siRNAs, conjugated or not with cholesterol on the 3' end as described (15), were from IDT. RNA sequences are provided in Supplementary Table S1. For some experiments the 3' end of the antisense strand was conjugated to Cy3, Alexa Fluor 647 or 750. The stability of RNAs incubated in human or mouse serum was assessed with aliquots removed during a 36-hour incubation at 37°C in 50% serum. Samples were analyzed by densitometry after polyacrylamide gel electrophoresis and ethidium bromide staining.

Fluorescence microscopy

Cells were incubated with 1 µmol/L Cy3-labeled EpCAM aptamer in microscopy chamber wells for indicated times and then counter stained with CellMask Deep Red Plasma Membrane Stain (Life Technologies) and imaged live. Images were acquired with a spinning disk confocal head (Yokogawa) coupled to a fully motorized epifluorescence microscope (Axio Observer) equipped with a 63× lens (Plan Apochromat, 1.4 NA, Carl Zeiss). Three 50 mW solid-state lasers (491, 561, and 660 nm; Cobalt Laser) were used as light sources. The imaging system operates under control of SlideBook 5.0 and an EM-CCD camera (Quant-EM, Hamamatsu) was used to acquire images.

Gene knockdown

For *in vitro* gene silencing experiments, cells were used immediately after plating at 10,000 cells per well in 96-well plates. For transfections, cells were incubated with lipoplexed siRNAs or AsiCs without lipid at 100 nmol/L or 4 µmol/L concentrations, respectively, unless otherwise indicated, in WIT-T or OptiMEM medium, respectively. For lipid transfections, cells were transfected with Dharmafect I according to the manufacturer's protocol. Gene knockdown was assessed by measuring protein levels using flow cytometry 72 to 96 hours after treatment and by measuring mRNA by qRT-PCR 24 to 48 hours after treatment. Cell viability was assessed by CellTiter-Glo (Promega) or by Trypan Blue staining 24 to 48 hours after treatment.

Ago immunoprecipitation

MB468 cells (10⁶ cells/well of a 6-well plate) were treated with 4 µmol/L *PLK1* AsiCs or unconjugated *PLK1* siRNA for 48 hours. The cytoplasmic lysates of AsiC/siRNA-treated cells were incubated with protein G Dynabeads (Life Technologies) that were coated with 2 µg anti-pan-Ago antibody (clone 2A8, Millipore) or mouse IgG overnight at 4°C in the presence of RNase inhibitors (Life Technologies) and protease inhibitors (Roche). The beads were washed 5 times with NT2 buffer (50 mmol/L Tris pH 7, 150 mmol/L NaCl, 0.05% NP-40) and eluted by incubation for 30 minutes at 55°C with 200 µL SDS-TE buffer (5 mmol/L Tris pH 7.5, 0.5 mmol/L EDTA, 0.5% SDS). RNA was extracted from the unbound supernatants and bead-bound protein-RNA complexes eluted from the beads using TRIzol LS (Life Technologies). Taq-Man small RNA assay kits that included predesigned primers (Life Technologies) were used to quantify *PLK1* siRNA and miR-16 by qRT-PCR according to the manufacturer's manual. The amount of *PLK1* siRNA in the supernatant and immunoprecipitates was normalized to miR-16.

qRT-PCR

Total RNA was extracted with TRIzol (Invitrogen) and cDNA prepared from 1,000 ng total RNA using the ThermoScript RT Kit

(Invitrogen) as per the manufacturer's directions. qPCR of cDNAs was performed using SYBR Green Master Mix (Applied Biosystems) and a Bio-Rad C1000 Thermal Cycler (Bio-Rad). Relative C_t values were normalized to *GAPDH*. Primers are provided in Supplementary Table S1.

Flow cytometry

Cells were stained in PBS containing 0.5% fetal calf serum, 1 mmol/L EDTA, and 25 mmol/L HEPES with the following antibodies: EpCAM (Clone EBA-1 from BD Biosciences or clone 9C4 from BioLegend), AKT1 (clone 55/PKBa/Akt from BD Biosciences). Flow cytometry analysis was performed on a FACS-Canto II (BD Biosciences) using FlowJo (Treestar Inc.) software.

RNA uptake by human breast tissues

Fresh breast cancer and normal breast tissue biopsies, obtained from the UMASS Tissue Bank, were cut into $3 \times 3 \times 3$ mm cubes and placed in 96 well plates containing 100 μ L RPMI. Samples were incubated for 24 hours with 4 μ mol/L Alexa647-labeled siRNA, 100 nmol/L Alexa647-labeled, chol-siRNA, or 4 μ mol/L Cy3-labeled EpCAM-AsiC, all targeting *eGFP*, and photographed. To make single-cell suspensions, triplicate samples were pooled, sonicated using a gentleMACS dissociator (Miltenyi, spleen program for 30 minutes at 37°C), incubated at 37°C for 30 minutes with shaking in 10 mL RPMI containing 1 mg/mL collagenase II (Sigma-Aldrich), and then sonicated again. The resulting cell suspension was passed through a 70 μ m cell strainer (BD Falcon), washed with 30 mL RPMI, and stained for flow cytometry.

TIC *in vitro* assays

For colony forming assay, 1,000 cells were treated for 6 hours with medium, 4 μ mol/L AsiC or 100 nmol/L paclitaxel (Sigma) in round-bottom 96-well plates and transferred to 10 cm plates in serum-containing medium. Medium was replaced every 3 days. After 8 to 14 days, cells were fixed in methanol (-20°C) and stained with crystal violet. For sphere formation assay, cells (1,000/mL), treated as above for 6 hours in round-bottom 96-well plates, were cultured in suspension in serum-free DMEM/F12 1:1 (Invitrogen), supplemented with EGF (20 ng/mL, BD Biosciences), B27 (1:50, Invitrogen), 0.4% bovine serum albumin (Sigma), and 4 μ g/mL insulin (Sigma). Spheres were counted after 1 to 2 weeks.

Mouse experiments

All animal experiments were performed with the approval of the Harvard Medical School and Boston Children's Hospital Animal Care and Use Committees. Eight-week-old female Nu/J mice (Stock # 002019, Jackson Laboratories) were used for all experiments.

To assess tumor initiation, mice were injected subcutaneously with MB468-luc (5×10^6 viable cells) that had been pretreated for 24 hours with medium or 4 μ mol/L EpCAM-AsiCs targeting *eGFP* or *PLK1*. Cells were trypsinized with TrypLE Express (Invitrogen), resuspended in WIT media, and injected subcutaneously in the flank. After intraperitoneal injection of 150 mg/kg D-luciferin (Caliper Life Sciences), luminescent images of the whole body were taken every 5 days for 15 days using an IVIS Spectrum using Living Image software (Caliper Life Sciences). The mice were sacrificed on day 15.

To assess AsiC uptake, MB468-luc (5×10^6) and MB231-luc-mCherry (5×10^5) cells trypsinized with TrypLE Express (Invi-

trogen), were resuspended in 1:1 WIT-Matrigel and injected subcutaneously in opposing flanks. Five days later, when tumors were easily palpated, mice were injected subcutaneously in the neck with Alexa750-EpCAM-AsiC-GFP (0.5 mg/kg in PBS). Animals were maintained on an alfalfa-free diet (Research Diets, Inc) to reduce autofluorescence and imaged using the IVIS Spectrum 15 minutes after the injection and twice thereafter at 2-day intervals. Animals were sacrificed 4 days after treatment and tumors were excised and imaged.

To assess tumor inhibition, MB468-luc (5×10^6) and MB231-luc-mCherry (5×10^5) cells trypsinized with TrypLE Express (Invitrogen), resuspended in 1:1 WIT-Matrigel, were injected subcutaneously in opposite flanks. Five days later, when tumors were palpable, mice bearing tumors of comparable size were randomized into groups and treated subcutaneously every 3 days in the scruff of the neck with PBS containing nothing or 5 mg/kg EpCAM-AsiCs directed against *eGFP* or *PLK1*, EpCAM aptamer, or *PLK1* siRNA. Mice were sacrificed on day 13. A similar protocol was followed in mice injected with 4×10^4 MCF10-CA1a-Luc cells, except that treatment was initiated 1 day after tumors were implanted, the injections were performed in the flank near the tumor, but not intratumorally, and the mice were sacrificed on day 15.

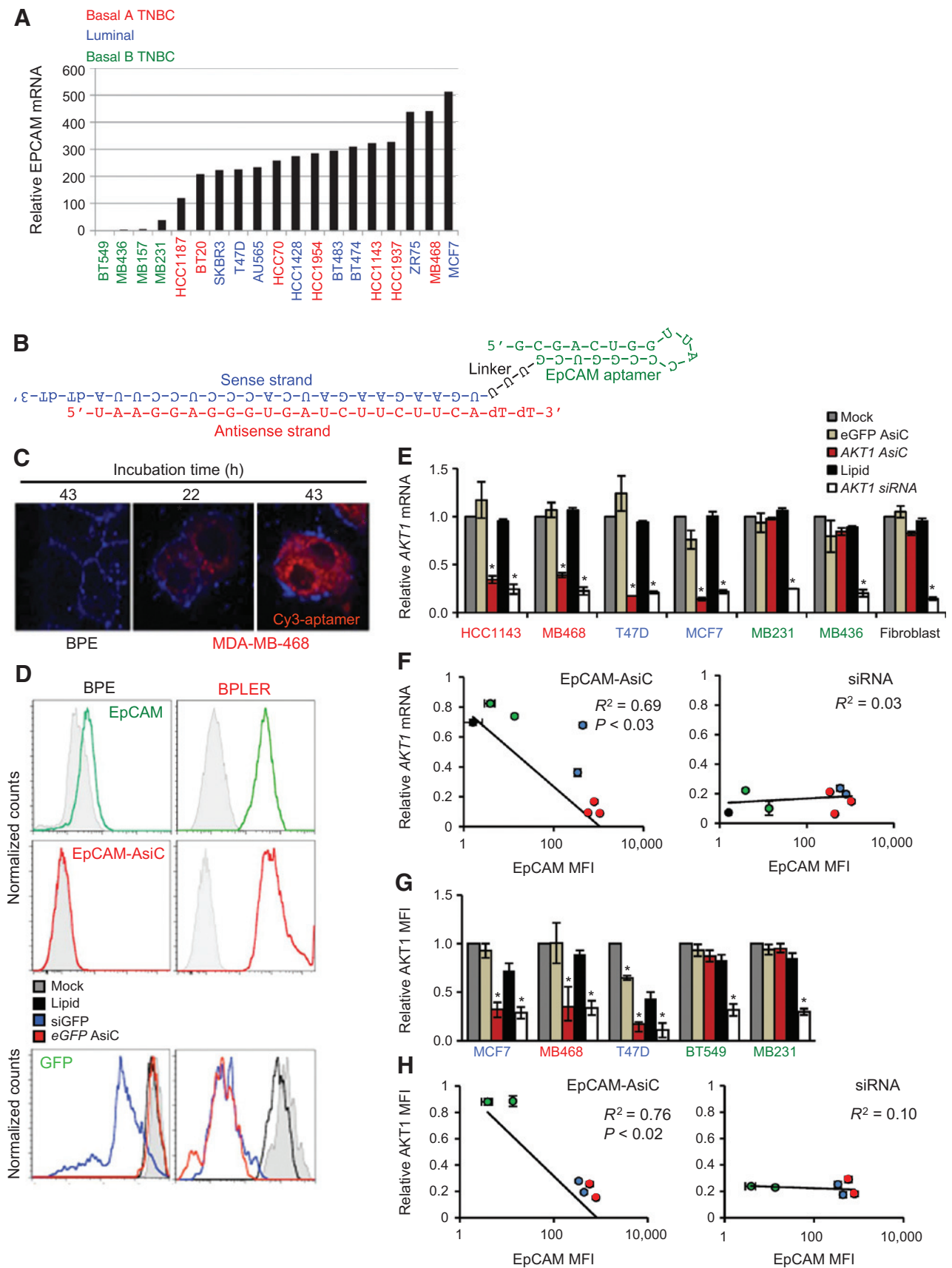
Statistical analysis

Student *t* tests were used to analyze the significance between the treated samples and the controls where the test type was set to two-tailed distribution and two-sample equal variance. To assess innate immune stimulation, one-way ANOVA with Bonferroni multiple comparison test was performed using GraphPad Prism 4 software (GraphPad Software). $P < 0.05$ was considered statistically significant. Correlations were analyzed by Pearson coefficient.

Measurement of *in vivo* innate immune stimulation

Mice were injected sc with *eGFP* EpCAM-AsiCs (5 mg/kg) or intraperitoneally with Poly(I:C; 5 or 50 mg/kg). Serum samples, collected at baseline and 6 and 16 hours after treatment, were stored at -80°C before measuring IFN β , IL6, and IP10 using the ProcartaPlex Multiplex Immunoassay (Affymetrix/eBioscience). Splens, harvested at sacrifice 16 hours after treatment, were stored in RNAlater (Qiagen) before extracting RNA by adding TRIzol (Invitrogen) to single-cell suspensions generated using the gentleMACS Dissociator (MACS Miltenyi Biotec). cDNA was synthesized using Superscript III and random hexamers (Invitrogen) and PCR was performed using SsoFast EvaGreen Supermix and a Bio-Rad CFX96 Real-Time PCR System (Bio-Rad Laboratories) using the following primers:

Gapdh forward: 5'- TTCACCACCATGGAGAAGGC-3',
Gapdh reverse: 5'- GGCATGGACTGTGGTCATGA-3',
ifnb forward: 5'-CTGGAGCAGCTGAATGGAAAAG-3',
ifnb reverse: 5'- CTTGAAGTCCGCCCTGTAGGT-3',
il-6 forward: 5'-TGCCCTTCATTTATCCCTTGAA-3',
il-6 reverse: 5'-TTACTACATTCAGCCAAAAGCAC-3',
ip-10 forward: 5'-GCTGCCGTCAATTTCTGC-3',
ip-10 reverse: 5'-TCTCACTGGCCCGTCATC-3',
oas-1 forward: 5'-GGAGTTGCAGTGCCAACGAAG-3',
oas-1 reverse: 5'-TGGAAGGGAGGCAGGGCATAAC-3',
stat1 forward: 5'-TTTGCCAGACTCCAGCTCCTG-3',
stat1 reverse: 5'-GGGTGCAGGTTCCGGGATTCAAC-3'.



Results

EpCAM is highly expressed on epithelial breast cancer cell lines

We first examined EpCAM expression in breast cancer cell lines. On the basis of gene expression data in the Cancer Cell Line Encyclopedia (40), EpCAM mRNA is highly expressed in basal-A TNBC and luminal breast cancer cell lines, but poorly in basal-B (mesenchymal) TNBCs (Fig. 1A; in all figure labels in this article, basal-A TNBC cell lines are labeled in red, basal-B TNBC in green, and luminal cell lines in blue.) Surface EpCAM staining, assessed by flow cytometry, was 2 to 3 logs brighter in all luminal and basal-like cell lines tested, than in normal epithelia immortalized with hTERT (BPE; ref. 41), fibroblasts, or mesenchymal TNBCs (Table 1). Thus, EpCAM is highly expressed in epithelial breast cancer cell lines compared with normal cells or mesenchymal tumors.

EpCAM-AsiCs selectively knock down gene expression in EpCAM⁺ breast cancer cells

A 19 nucleotide (nt) aptamer that binds to human EpCAM with 12 nmol/L affinity (19) was identified by SELEX (42, 43). A handful of EpCAM-AsiCs that linked either the sense or antisense strand of the siRNA to the 3'-end of the aptamer by several linkers were designed and synthesized with 2'-fluoropyrimidine substitutions and 3'-dTdT overhangs to enhance *in vivo* stability, avoid off-target knockdown of partially complementary genes, and limit innate immune receptor stimulation. To test RNA delivery, gene knockdown, and antitumor effects, siRNAs were incorporated to knock down a marker gene (*eGFP*), a ubiquitous, endogenous nonessential gene (*AKT1*), and *PLK1*, a kinase required for mitosis, whose knockdown is lethal to dividing cells (Supplementary Table S1). The AsiC that performed best in dose response studies of gene knockdown joined the 19 nt EpCAM aptamer to the sense (inactive) strand of the siRNA via a U-U-U linker (Fig. 1B). The EpCAM-AsiC was produced by annealing the chemically synthesized approximately 42–44 nt long strand (19 nt aptamer + linker + 20–22 nt siRNA sense strand) to a 20–22 nt antisense siRNA strand. The 2'-fluoropyrimidine modification led to RNase resistance and stability in 50% human serum ($t_{1/2} \gg 36$ hours, Supplementary Fig. S1). EpCAM-AsiCs did not trigger innate immunity when injected sc into tumor-bearing mice (Supplementary Fig. S2).

To verify selective uptake by EpCAM⁺ tumor cells, we first used confocal fluorescence microscopy to compare internalization of the EpCAM aptamer, fluorescently labeled at the 5'-end with Cy3, in EpCAM⁺ MDA-MB-468 TNBC cells and BPE, EpCAM^{dim} immortalized breast epithelial cells (Fig. 1C). Because AsiCs contain only one aptamer, they do not crosslink the receptor

Table 1. EpCAM protein expression on breast cancer cells, immortalized normal breast epithelial cells, and normal human fibroblasts, assessed by flow cytometry (MFI, mean fluorescence intensity)

Cell line	Subtype	EpCAM MFI
BPE	Immortalized normal epithelium	2
BPLER	Basal-A TNBC	109
HMLER	Unclassified TNBC (myoepithelial)	72
HCC1143	Basal-A TNBC	1,068
HCC1937	Basal-A TNBC	806
HCC1187	Basal-A TNBC	289
HCC1806	Basal-A TNBC	558
HCC70	Basal-A TNBC	443
MB468	Basal-A TNBC	340
MCF7	Luminal	583
T47D	Luminal	799
BT549	Basal-B TNBC	2
MB231	Basal-B TNBC	31
MB436	Basal-B TNBC	4
Human fibroblast	Normal tissue	14

they recognize. As a consequence, cellular internalization is slow as it likely occurs via receptor recycling, rather than the more rapid process of activation-induced endocytosis. Only MDA-MB-468 cells took up the aptamer. Uptake was clearly detected at 22 hours, but increased greatly after 43 hours. To test whether EpCAM-AsiCs are specifically taken up by EpCAM bright cell lines, the 3' end of the antisense strand of the AsiC was fluorescently labeled. EpCAM⁺ BPLER, a basal-A TNBC cell line transformed from BPE by transfection with human *TERT*, SV40 early region and *H-RAS*^{V12}, took up Alexa-647 EpCAM-AsiCs when analyzed after a 24-hour incubation, but BPE cells did not (Fig. 1D). Previous studies have shown that AsiCs are processed within cells by Dicer to release the siRNA from the aptamer (10, 12, 15). To verify that the released siRNA was taken up by the RNA-induced silencing complex (RISC), we used qRT-PCR to amplify *PLK1* siRNA immunoprecipitated with Ago when MDA-MB-468 cells were incubated with *PLK1* EpCAM-AsiCs (Supplementary Fig. S3). No *PLK1* siRNA bound to Ago when the same cells were incubated with *PLK1* siRNAs.

Next to assess whether gene knockdown was specific to EpCAM⁺ tumors, we compared *eGFP* knockdown by *eGFP* EpCAM-AsiCs and lipid transfection of *eGFP* siRNAs in BPE and BPLER cell lines, which stably express *eGFP* (Fig. 1D). Although transfection of *eGFP* siRNAs knocked down gene expression equivalently in BPE and BPLER, incubation with EpCAM-AsiCs in the absence of any transfection lipid selectively knocked down expression only in BPLER. AsiC knockdown was uniform and

Figure 1.

EpCAM-AsiCs knock down gene expression specifically in EpCAM⁺ epithelial breast cancer cells. A, EpCAM mRNA expression in epithelial basal-A TNBC (red) and luminal (blue) breast cancer cell lines versus mesenchymal basal-B TNBC (green) cell lines. Data from the Cancer Cell Line Encyclopedia (40). B, design of *PLK1* EpCAM-AsiC, containing an EpCAM aptamer linked to the sense strand of a *PLK1* siRNA, which is annealed to the antisense strand of the siRNA. The AsiC long strand was chemically synthesized with 2'-fluoropyrimidines. C, fluorescence microscopy comparison of uptake of Cy3-labeled EpCAM aptamer (red) by the basal-A TNBC cell line MDA-MB-468 and the immortalized epithelial cell line BPE (41). Plasma membrane is counter stained (blue). D, EpCAM expression (top), uptake of Alexa-647-labeled EpCAM-AsiC (middle) and *eGFP* knockdown by *eGFP* EpCAM-AsiC or transfected *eGFP* siRNA (bottom) in basal-A TNBC cell line BPLER and immortalized breast epithelial cell line BPE. Uptake was assessed 24 hours after incubation and knockdown was assessed 3 days after incubation. Data are representative of 3 independent experiments. Gray histograms in top and middle panels are unstained and mock-treated cells, respectively. E–H, *AKT1* mRNA, assessed by qRT-PCR relative to *GAPDH* mRNA (E and F), and protein, assessed by flow cytometry (G and H), measured 3 days after indicated incubation with AsiCs or with lipid-complexed siRNAs. Controls were mock and transfection lipid-treated cells. The cancer cell line subtypes are color coded in the labels as in A. E and G, mean \pm SEM of 3 independent experiments; *, $P < 0.05$, two-tailed Student *t* test. F and H, correlation between gene knockdown and EpCAM mean fluorescence intensity (MFI) after treatment with *AKT1* EpCAM-AsiC (left) or *AKT1* siRNA lipoplexes (right).

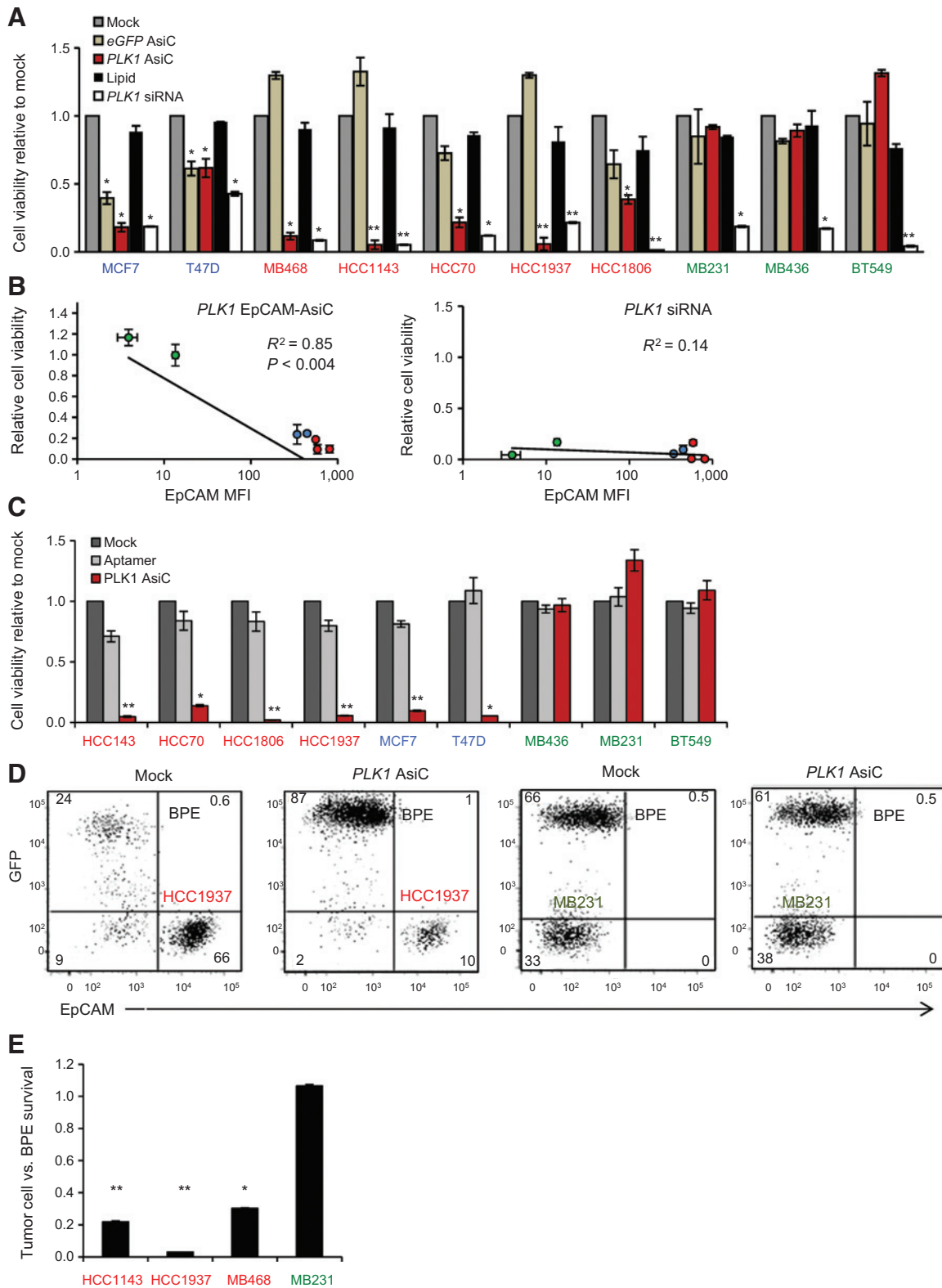


Figure 2. EpCAM-AsiCs targeting PLK1 specifically kill EpCAM⁺ breast cancer cells. A and B, breast cancer cell lines [luminal (blue), basal-A TNBC (red), basal-B TNBC (green)] were incubated with EpCAM-AsiCs targeting *eGFP* or *PLK1* or with lipoplexed *PLK1* siRNAs (or with medium or transfection lipid as controls). Cell viability was assessed by Cell-TiterGlo 1 day later. Mean \pm SEM of 3 independent experiments is shown in A and correlation between cell viability after incubation with *PLK1* EpCAM-AsiCs (left) or *PLK1* siRNAs (right) and EpCAM MFI is shown in B. C, breast cancer cell lines were incubated with medium (mock), EpCAM aptamer, or *PLK1* EpCAM-AsiC and cell viability was assessed 1 day later. (Continued on the following page.)

comparable to that achieved with lipid transfection. Next, we compared the knockdown of *AKT1* by *AKT1* AsiCs and transfected *AKT1* siRNAs in 6 breast cancer cell lines and normal human fibroblasts (Fig. 1E). *AKT1* was selectively knocked down by EpCAM-AsiCs targeting *AKT1* only in EpCAM^{bright} luminal and basal-A TNBCs, but not in mesenchymal basal-B TNBCs or fibroblasts. As expected, AsiCs targeting *eGFP* had no effect on *AKT1* levels and transfection of *AKT1* siRNAs comparably knocked down expression in all the cell lines studied. Moreover, EpCAM-AsiC knockdown of *AKT1* correlated with EpCAM expression (Fig. 1F). Similar results were obtained when *AKT1* protein was analyzed by flow cytometry in stained transfected cells (Fig. 1G and H). Thus, *in vitro* knockdown by EpCAM-AsiCs is effective and specific for EpCAM^{bright} tumor cells.

PLK1* EpCAM-AsiCs selectively kill EpCAM^{bright} tumor cells *in vitro

To explore whether EpCAM-AsiCs could be used as antitumor agents in breast cancer, we examined by CellTiterGlo assay the effect of AsiCs directed against *PLK1*, a kinase required for mitosis, on survival of 10 breast cancer cell lines that included 5 basal-A TNBCs, 2 luminal cell lines, and 3 basal-B TNBCs. EpCAM-AsiCs targeting *PLK1*, but not control AsiCs directed against *eGFP*, decreased cell proliferation in the basal-A and luminal cell lines, but did not inhibit basal-B cells (Fig. 2A). Lipid transfection of *PLK1* siRNAs suppressed the growth of all the cell lines. The antiproliferative effect strongly correlated with EpCAM expression (Fig. 2B). To determine whether ligation of the EpCAM aptamer contributed to the antiproliferative effect of the EpCAM-AsiC, we compared survival of cells treated with *PLK1* EpCAM-AsiCs with cells treated with the aptamer on its own (Fig. 2C). The aptamer by itself did not reproducibly affect survival of any breast cancer cell lines, possibly because as a monomeric agent it does not cross-link the EpCAM receptor to alter EpCAM signaling. Thus, the *PLK1* EpCAM-AsiC asserts its specific antitumor effect on EpCAM⁺ breast cancer cells by gene knockdown.

To determine whether EpCAM-AsiCs specifically target EpCAM⁺ cells when mixed with EpCAM^{dim} nontransformed epithelial cells, we incubated cocultures of GFP⁻ TNBC cells and GFP⁺ BPE cells with *PLK1* EpCAM-AsiCs or medium and used GFP fluorescence to measure their relative survival by flow cytometry 3 days later (Fig. 2D and E). EpCAM-AsiCs targeting *PLK1* greatly reduced the proportion of surviving EpCAM⁺ basal-A tumor cells, but had no effect on survival of an EpCAM⁻ basal-B cell line. Thus, *PLK1* EpCAM-AsiCs are selectively cytotoxic for EpCAM⁺ tumor cells when mixed with normal cells.

EpCAM-AsiCs concentrate in EpCAM⁺ breast tumor biopsy specimens

We next examined whether EpCAM-AsiCs concentrate in human breast tumors relative to normal breast samples within intact tissues. Paired normal tissue and breast tumor biopsies

from 3 breast cancer patients (2 ER⁺PR⁺HER2⁻ luminal breast cancers, 1 TNBC) were cut into approximately 3 mm sided cubes and placed in 96-well plates. The tumor sample cells were all EpCAM^{bright} and the normal tissue cells were EpCAM^{dim} (Fig. 3A). Fluorescently labeled Alexa647-siRNAs (not expected to be taken up by either normal tissue or tumor), Alexa647-cholesterol-conjugated siRNAs (chol-siRNAs, expected to be taken up by both), or Cy3-EpCAM-AsiCs were added to the culture medium and the tissues were incubated for 24 hours before harvest. The Cy3 signal of the AsiC, visible to the naked eye, concentrated only in the tumor specimens and was not detected in normal tissue (Fig. 3B). To quantify RNA uptake, flow cytometry analysis was performed on washed single-cell suspensions of the tissue specimens [representative tumor-normal tissue pairs (Fig. 3C), mean \pm SEM of triplicate biopsies from 3 EpCAM^{bright}-paired breast tumor-normal tissue samples (Fig. 3D)]. The EpCAM-AsiC was significantly taken up by the tumors, but not normal tissue, while neither took up the unconjugated siRNA and both weakly took up the chol-siRNA. Thus, within intact tissue, EpCAM-AsiCs are selectively delivered to EpCAM^{bright} tumors relative to normal tissue.

***PLK1* EpCAM-AsiCs inhibit TICs of EpCAM⁺ tumors**

EpCAM was chosen for targeting in part because EpCAM marks TICs and metastasis-initiating cells (20, 22, 26, 27, 31). To investigate whether EpCAM-AsiCs inhibit TICs, we compared colony and mammosphere formation (TIC functional *in vitro* assays) after mock treatment, treatment with paclitaxel or with EpCAM-AsiCs against *eGFP* or *PLK1*. *PLK1* EpCAM-AsiCs more strongly inhibited colony and mammosphere formation of EpCAM⁺ basal-A TNBCs and luminal cell lines than paclitaxel, but were inactive against EpCAM⁻ basal-B TNBCs (Fig. 4A-C). TIC inhibition was specific, since *eGFP* AsiCs had no effect. To evaluate the effect of EpCAM-AsiCs on tumor initiation, EpCAM⁺ MB468 cells stably expressing luciferase were treated overnight with medium or *PLK1* or *eGFP* EpCAM-AsiCs and equal numbers of viable cells were then implanted subcutaneously in nude mice (Fig. 4D). *PLK1* EpCAM-AsiCs completely blocked tumor formation assessed by *in vivo* luminescence (Fig. 4E and F). Thus, *PLK1* EpCAM-AsiCs inhibit *in vitro* TIC assays and tumor initiation selectively for EpCAM⁺ breast cancers.

Subcutaneously administered EpCAM-AsiCs are selectively taken up by distant EpCAM⁺ TNBCs

To be clinically useful, EpCAM-AsiCs need to be taken up by disseminated tumor cells. Intravenously injected AsiCs do not accumulate efficiently within subcutaneous tumors implanted in the flanks of nude mice, probably because their size (~25 kDa) is below the threshold for kidney filtration and they are rapidly excreted. Linkage to polyethylene glycol greatly enhanced the circulating half-life, tumor accumulation, and antitumor therapeutic effect of PSMA-AsiCs in a mouse xenograft model of prostate cancer (11). However, to see if this modification could

(Continued.) Mean \pm SEM of 3 independent experiments is shown. In A and C, *, $P < 0.05$; **, $P < 0.01$, relative to mock control by two-tailed Student *t* test. D and E, an equal mixture of GFP-TNBC cells (red, basal-A; green, basal-B) and immortalized GFP⁺ normal breast epithelial cells (BPE) were untreated or treated with *PLK1* EpCAM-AsiCs and analyzed for survival by flow cytometry 3 days later. Shown are representative flow cytometry plots (D) and survival (E) of the TNBC cell line relative to BPE (mean \pm SEM of 4 independent experiments; *, $P < 0.05$; **, $P < 0.01$, relative to the MB231 basal-B-cell line by two-tailed Student *t* test).

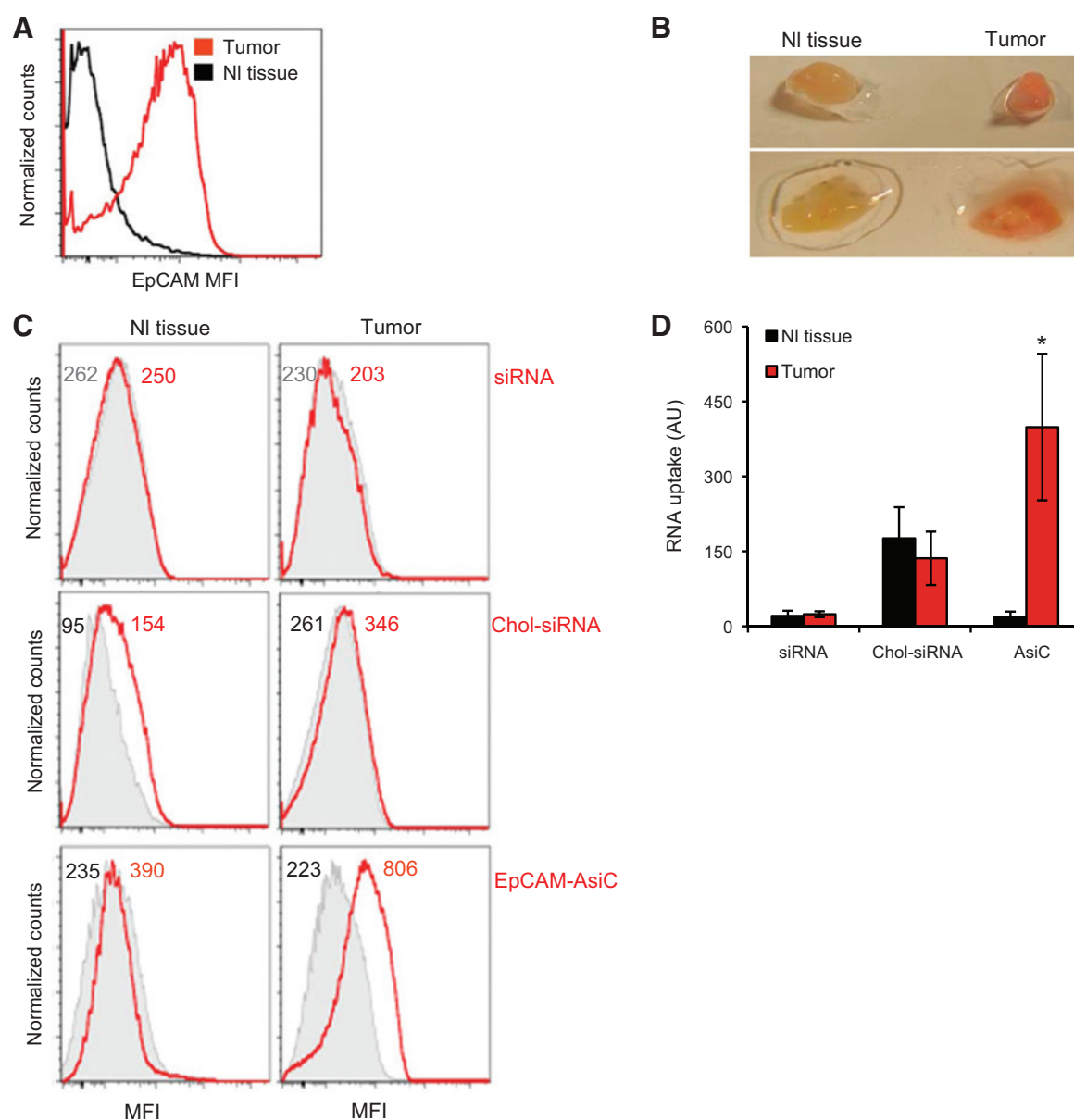


Figure 3. Human breast cancer tissues specifically take up Cy3-labeled EpCAM-AsiCs. A, single-cell suspensions of a human basal-A TNBC tumor biopsy and adjacent normal tissue were analyzed by flow cytometry for EpCAM expression. B–D, two luminal and one basal-A TNBC human biopsy and adjacent normal tissue were incubated with eGFP Cy3-EpCAM-AsiCs, Alexa647-labeled siRNAs or chol-siRNAs for 24 hours, photographed (B) and digested to a single-cell suspension and analyzed by flow cytometry for RNA uptake (C and D). Cy3 is visible to the naked eye. B and C, results for the basal-A TNBC sample; D, the mean \pm SEM uptake of 3 replicates of 3 patient samples. C, gray histograms and numbers (MFI) represent untreated samples; red histograms and numbers, fluorescence after indicated treatment. (*, $P < 0.05$, Student *t* test of tumor vs. normal tissue).

be bypassed, we examined by live animal epifluorescence imaging whether sc injection of Alexa750-labeled eGFP EpCAM-AsiCs in the scruff of the neck of 7 mice led to accumulation in distant EpCAM⁺ MB468 and EpCAM⁻ MB231 TNBCs implanted subcutaneously in each flank (Fig. 5). Within a day of injection, EpCAM-AsiCs concentrated in the EpCAM⁺ tumor and persisted there for at least 4 days. The EpCAM-AsiCs were detected around the injection site on day 2, but were only found within the EpCAM⁺ tumor on day 4.

PLK1 EpCAM AsiCs cause regression of basal-A TNBC and Her2 breast cancer xenografts

Because subcutaneously injected EpCAM-AsiCs concentrated in distant EpCAM⁺ tumors, we next looked at whether subcutaneous injection of PLK1 EpCAM-AsiCs could selectively inhibit the growth of an EpCAM⁺ TNBC xenografted tumor. EpCAM⁺ MB468-luc cells were implanted in Matrigel in one flank of a nude mouse and EpCAM⁻ MB231-luc-mCherry cells were implanted on the opposite flank. Once the luciferase

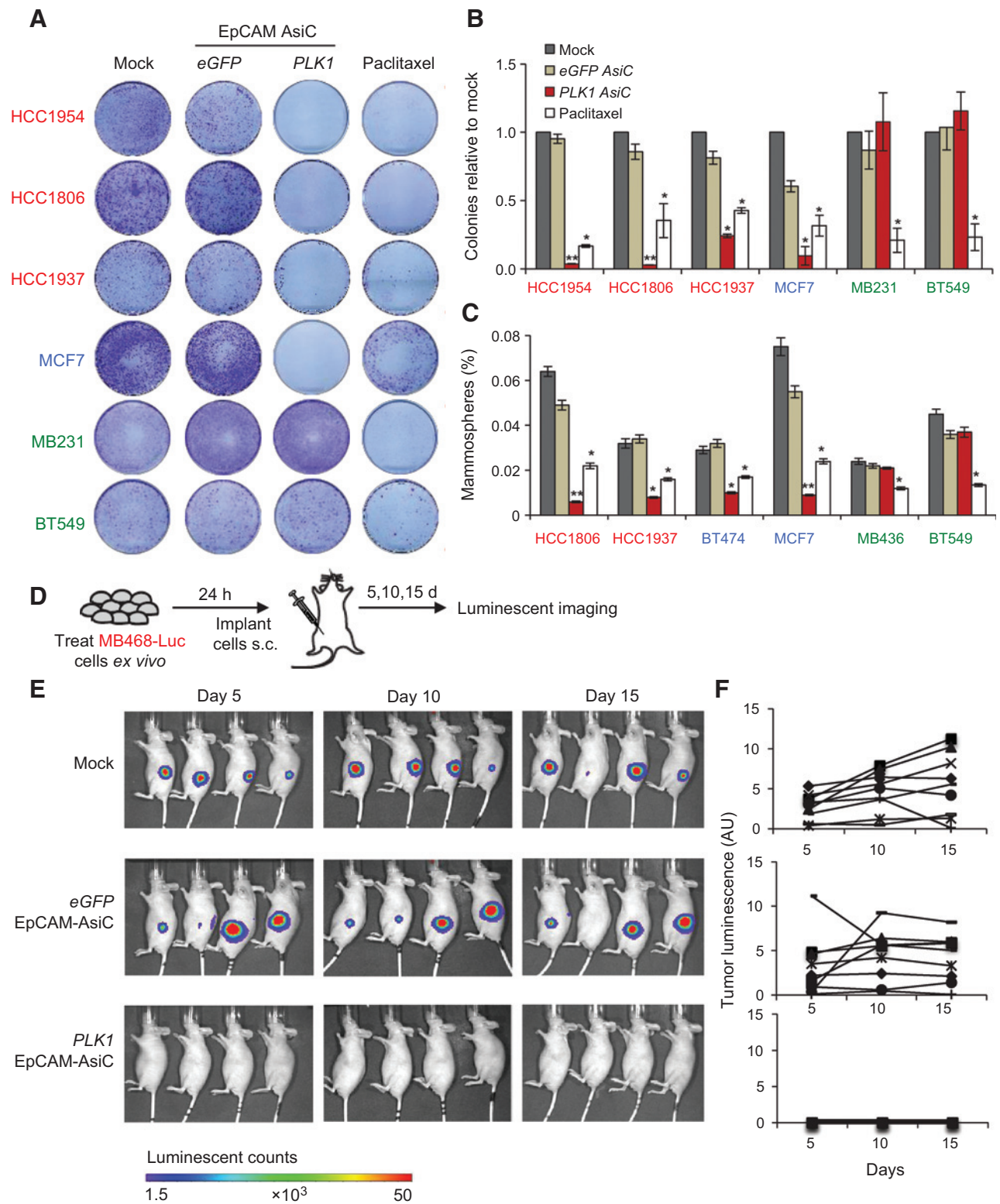


Figure 4. *PLK1* EpCAM-AsiCs inhibit tumor initiation of EpCAM⁺ breast cancer cells. A–C, human breast cancer cell lines [luminal (blue), basal-A TNBC (red), basal-B TNBC (green)] were untreated or treated with *eGFP* or *PLK1* EpCAM-AsiCs or paclitaxel for 24 hours and washed free of drug before assessing colony formation (A and B) and mammosphere assay (C). A, representative colony-forming assay; B and C, mean \pm SEM of 3 independent experiments (*, $P < 0.05$; **, $P < 0.01$, Student *t* test vs. untreated sample). D–F, MB468-luc cells, untreated or treated for 24 hours with *eGFP* or *PLK1* EpCAM-AsiCs, were injected subcutaneously in the flanks of nude mice ($n = 9$). Mice were imaged every 5 days. D shows experimental scheme, E shows luciferase images of representative mice, and F shows luminescence of all mice. AU, arbitrary units.

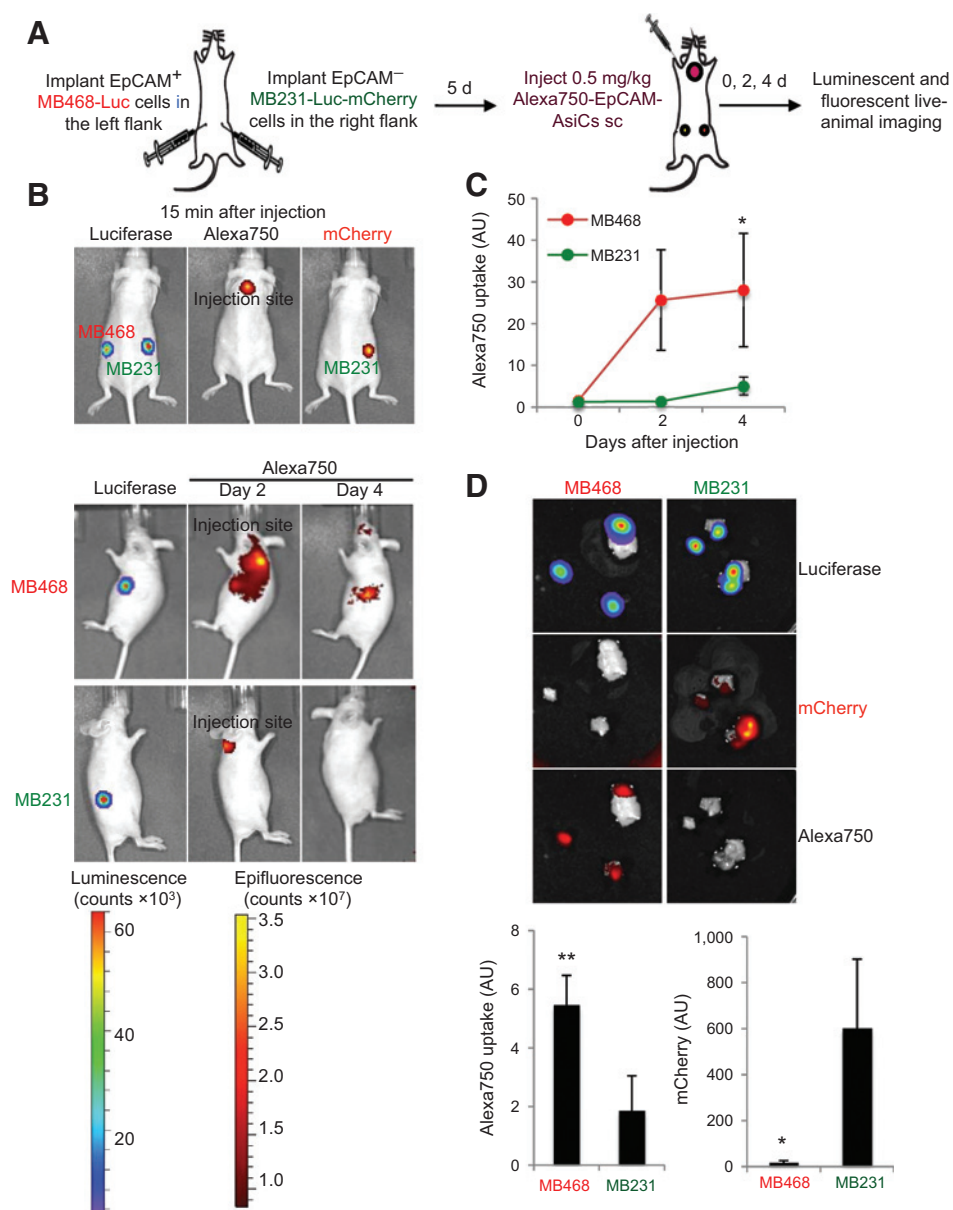
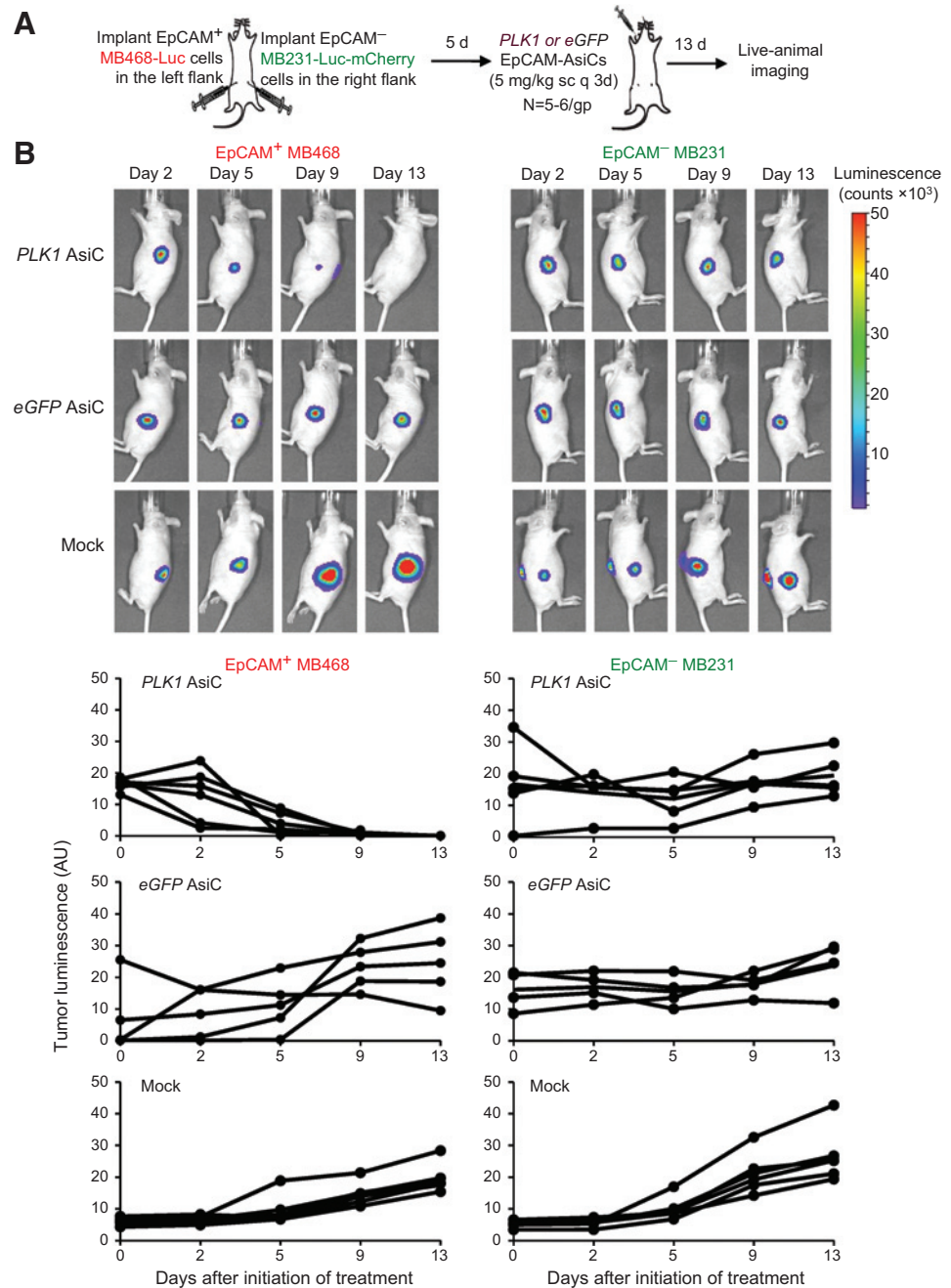


Figure 5. Alexa750-EpCAM-AsiCs are taken up by EpCAM⁺ tumors. A, experimental schema ($n = 7$ or 8). B and C, luminescent and fluorescent images of representative treated mice [side views show indicated EpCAM+mCherry-basal-A tumor (red) and EpCAM-mCherry+ basal-B tumor (green)]. C, shows Alexa 750 tumor uptake (mean \pm SEM; *, $P < 0.05$) in all treated mice. D, images of harvested tumors removed 4 days after treatment (top) and mean \pm SEM of Alexa 750 and mCherry signals in excised tumors (bottom). AU, arbitrary units (*, $P < 0.05$; **, $P < 0.01$; by two-tailed Student t test comparing EpCAM⁺ to EpCAM⁻ tumors).

signal of both tumors was clearly detected above background, groups of 5 to 6 mice were mock treated or injected subcutaneously with 5 mg/kg of EpCAM-AsiCs targeting *PLK1* or *eGFP* every 3 days for 2 weeks (we chose biweekly dosing because gene knockdown in siRNA-transfected rapidly dividing cancer cells usually only persists for about 5 days). Tumor growth was followed by luminescence. All the EpCAM⁺ tumors rapidly completely regressed only in mice that received the *PLK1*-targeting AsiCs (Fig. 6). The EpCAM⁺ tumors in mice treated with *eGFP*-targeting AsiCs and all the EpCAM⁻ tumors continued to grow. This experiment was repeated with similar results after injection of *PLK1* AsiCs into mice bearing Her2⁺ MCF10A-CA1a (Supplementary Fig. S4). Thus, subcutaneously injected *PLK1* EpCAM-AsiCs show specific antitumor activity against EpCAM⁺ human xenografts.

Discussion

Here we show that EpCAM-AsiCs can be used to knock down genes selectively in epithelial breast cancer cells and their stem cells, sparing normal epithelial cells and stroma, to cause tumor regression and suppress tumor initiation. In one very aggressive TNBC xenograft model, the EpCAM-AsiCs caused complete tumor regression after only 3 injections. However, we did not keep the mice alive off therapy to see if the tumors recurred after treatment was stopped. This is a flexible platform for targeted therapy, potentially for all the common epithelial cancers, which uniformly express high levels of EpCAM. Although we used EpCAM-AsiCs targeting *PLK1*, in principle, the siRNA could be varied to knock down any tumor dependency gene that would be customized to the tumor subtype or the molecular characteristics

**Figure 6.**

PLK1 EpCAM AsiCs inhibit growth of basal-A TNBC tumors. A, experimental schema; B, representative luciferase images and change in tumor luminescence of individual tumors (bottom). AU, arbitrary units.

of an individual patient's tumor. AsiC cocktails targeting more than one gene would be ideal for cancer therapeutics to lessen the chances of developing drug resistance. Targeted cancer therapy so far has relied on using tumor-specific antibodies or small-molecule inhibitors to oncogenic kinases. Although the AsiC platform is not new, using EpCAM as an AsiC ligand and developing RNAi therapy to target cancer stem cells is novel. No one before has shown that an unconjugated AsiC can have potent antitumor effects or that AsiCs could be administered subcutaneously (moreover, preliminary studies of sc administered CD4-AsiCs in humanized mice (L.A. Wheeler and J. Lieberman) showed strong knockdown in CD4 cells in the spleen and distant lymph nodes, suggesting that AsiCs targeting receptors on cells located else-

where in the body could also be administered subcutaneously). There is currently no targeted therapy for TNBC or for TICs. Targeted delivery has the advantage of reduced dosing and reduced toxicity to bystander cells. Developing targeted therapy for TNBC and developing ways of eliminating T-ICs are important unmet goals of cancer research.

Multiple groups have already used AsiCs to demonstrate impressive therapeutic effects (so far only in mice) to knock down gene expression in challenging types of cells, including cancer cells and lymphocytes. AsiCs are cleaved within cells by Dicer to liberate the siRNA from the aptamer (10, 12, 15). The U-U-U linker used here may be a particularly good Dicer substrate. AsiCs are an attractive method for gene knockdown outside the liver. It is

a flexible platform that by modifying the aptamer can be used to target any cell type and by changing the siRNA can be used to knock down any gene or combinations of genes. Over a thousand aptamers to human proteins have already been identified (44). Methods to select aptamers have become streamlined in recent years by combining deep sequencing and bioinformatics to more rapidly identify the features of active sequences (45). AsiCs are ideal for personalized therapy that can be altered to suit the molecular characteristics of an individual tumor or tumor subtype. The AsiC does not appear to activate the receptor, presumably because it does not crosslink it (15). AsiCs are a single chemical entity that is stable in the blood, simple to manufacture and not likely to be toxic. We did not see any evidence of toxicity or weight loss in treated mice, but we have not done formal testing. AsiCs, unlike liposomes and nanoparticles, do not get trapped in the liver and other filtering organs and should be able to readily penetrate tissues as well as small-molecule drugs (46, 47). EpCAM-AsiCs did not stimulate an innate immune response when injected *in vivo* and tested in the most sensitive immune cells (splenocytes) and at the time of a peak immune response with sensitive qRT-PCR assays. RNAs on their own do not induce antibodies, although the absence of AsiC antibodies needs to be formally tested. An aptamer drug, pegatanib (Macugen) is approved for macular degeneration and at least 8 aptamer drugs are in clinical trials, so aptamer RNAs on their own are well tolerated (48, 49).

The small size of the EpCAM aptamer used here is ideal for an AsiC drug, as RNAs <60 nt can be efficiently synthesized. Despite their promise, there is still considerable room to improve AsiCs, to optimize circulating $t_{1/2}$, cellular uptake, and endosomal release and to reduce the needed dose (although it is currently acceptable: approximately 1–5 mg/kg; refs. 11, 13, 15, 18). Recent studies have shown that the efficiency of GalNac-conjugated siRNAs in nonhuman primates can be improved by as much as 50-fold by optimizing the chemical modifications of the active strand to enhance stability and activity within the RNA-induced silencing complex (M. Manoharan, personal communication). Experiments to optimize the EpCAM-AsiCs are planned.

One potential source of toxicity of EpCAM-AsiCs could be targeting of epithelial tissue stem cells, especially in the gut. Because the EpCAM aptamer does not target mouse EpCAM, mouse experiments cannot adequately assess this possible toxicity. We will therefore need to use human tissues (or possibly primates) to look for EpCAM-AsiC toxicity to human tissue stem cells. An alternate drug development strategy would be to select

for an EpCAM aptamer that cross-reacts with mouse and human EpCAM.

In addition to their potential therapeutic use, EpCAM-AsiCs could also be a powerful *in vivo* research tool for identifying the dependency genes of tumors and TICs to define novel drug targets. In principle, aptamer chimeras could be designed to deliver not only siRNAs but also miRNA mimics or antagomirs, antisense oligonucleotides that function by other mechanisms besides RNAi, or even longer mRNAs or noncoding RNAs (50, 51). They could also be designed to incorporate more than one aptamer, multiple siRNAs, or even toxins or small-molecule anticancer drugs.

Disclosure of Potential Conflicts of Interest

J. Lieberman has ownership interest in Alnylam stock and is a member of the Alnylam Scientific Advisory Board. No potential conflicts of interest were disclosed by the other authors.

Authors' Contributions

Conception and design: L.A. Wheeler, J. Lieberman

Development of methodology: P. Hamar, M.T.N. Le, L.A. Wheeler

Acquisition of data (provided animals, acquired and managed patients, provided facilities, etc.): A. Gilboa-Geffen, P. Hamar, M.T.N. Le, L.A. Wheeler, A. Wittrup

Analysis and interpretation of data (e.g., statistical analysis, biostatistics, computational analysis): A. Gilboa-Geffen, P. Hamar, M.T.N. Le, F. Petrocca, A. Wittrup, J. Lieberman

Writing, review, and/or revision of the manuscript: P. Hamar, F. Petrocca, J. Lieberman

Administrative, technical, or material support (i.e., reporting or organizing data, constructing databases): P. Hamar, M.T.N. Le

Study supervision: L.A. Wheeler, J. Lieberman

Other (provided methodology for flow cytometry analysis of tissue samples and performed immunohistochemistry): R. Trifonova

Grant Support

This work was supported by a Department of Defense Breast Cancer Research Program (DOD BCRP) grant, (W81 XWH-09-1-0058; to J. Lieberman), Fulbright Visiting Scholar grant (1213204; to P. Hamar), Jane Coffin Childs Fund fellowship (to M. Le), Cancer Research Institute, Adelstein Fellowship, Harvard Medical School MD/PhD Program and Point Foundation fellowships to (L.A. Wheeler), Harvard CFAR scholar award (to R. Trifonova), DOD BCRP fellowship (to F. Petrocca), and Swedish Research Council fellowship (to A. Wittrup).

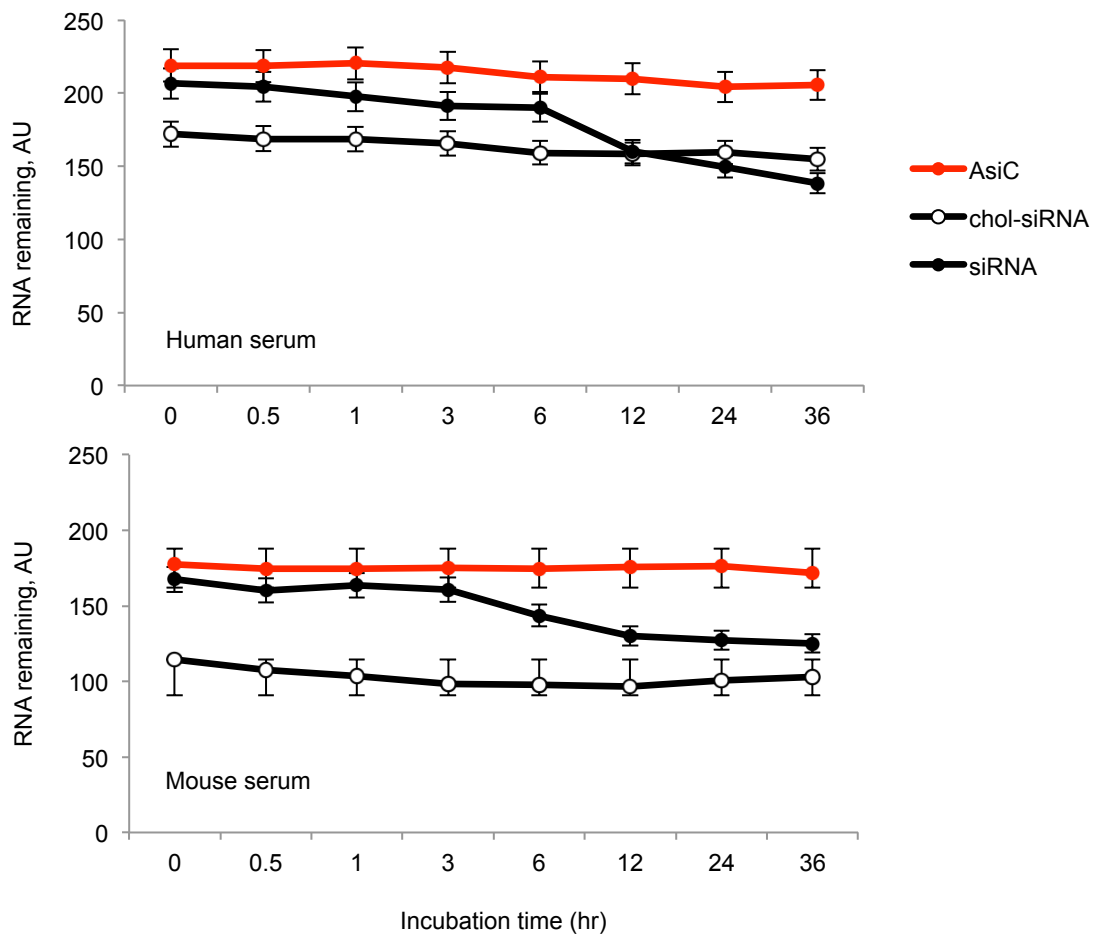
The costs of publication of this article were defrayed in part by the payment of page charges. This article must therefore be hereby marked *advertisement* in accordance with 18 U.S.C. Section 1734 solely to indicate this fact.

Received March 11, 2015; revised July 20, 2015; accepted August 3, 2015; published OnlineFirst August 11, 2015.

References

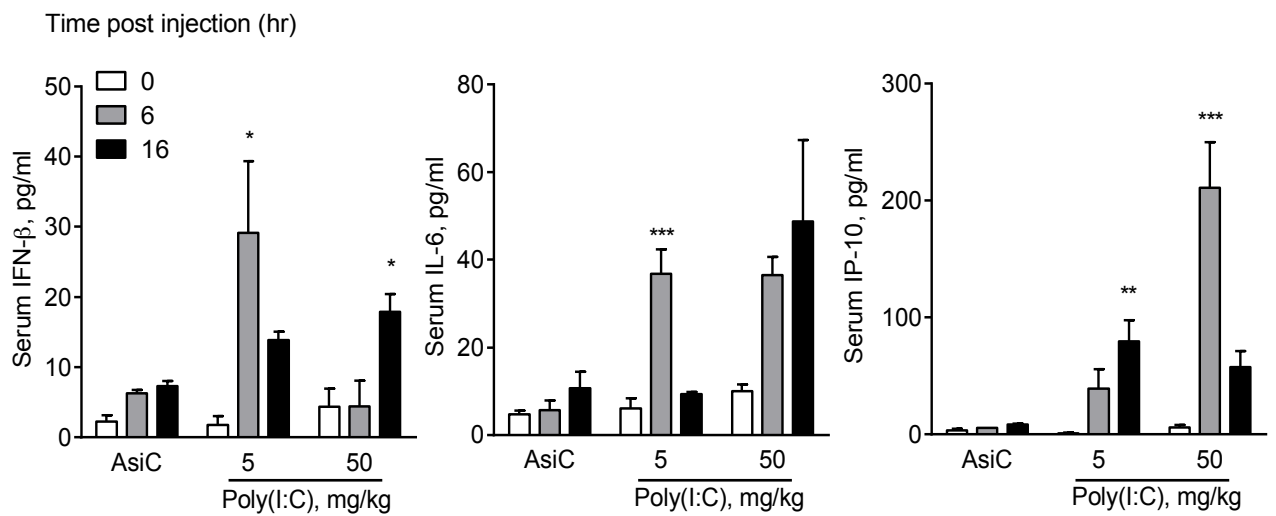
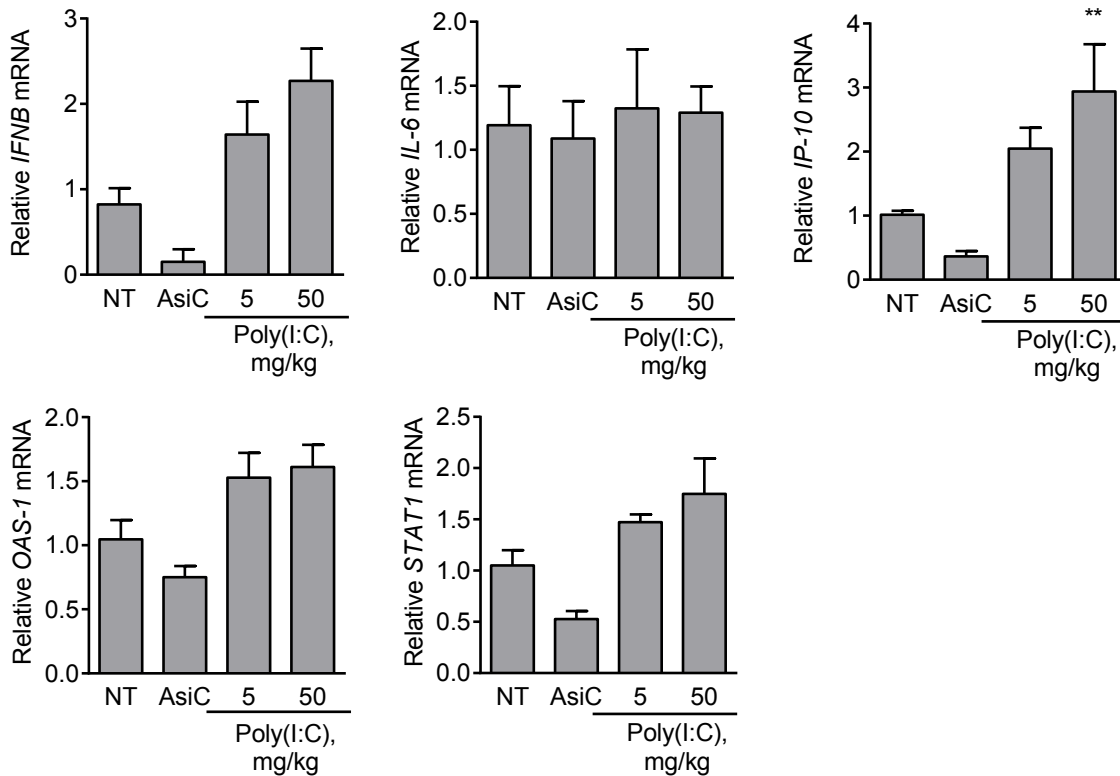
- de Fougerolles A, Vornlocher HP, Maraganore J, Lieberman J. Interfering with disease: a progress report on siRNA-based therapeutics. *Nat Rev Drug Discov* 2007;6:443–53.
- Tabernero J, Shapiro GI, LoRusso PM, Cervantes A, Schwartz GK, Weiss GJ, et al. First-in-humans trial of an RNA interference therapeutic targeting VEGF and KSP in cancer patients with liver involvement. *Cancer Discov* 2013;3:406–17.
- Adams D, Coehlo T, Suhr O, Conceicao I, Waddington-Cruz M, Schmidt H, et al. Interim Results for Phase II Trial of ALN-TTR02, a Novel RNAi Therapeutic for the Treatment of Familial Amyloidotic Polyneuropathy. Biennial Meeting of the Peripheral Nerve Society, St Malo, France 2013. [updated 2013 Jun 30; cited 2015 Aug 23]. Available from: <http://www.alnylam.com/capella/presentations/aln-trr02phiidata/>.
- Fitzgerald K, Frank-Kamenetsky M, Shulga-Morskaya S, Liebow A, Bettencourt BR, Sutherland JE, et al. Effect of an RNA interference drug on the synthesis of proprotein convertase subtilisin/kexin type 9 (PCSK9) and the concentration of serum LDL cholesterol in healthy volunteers: a randomised, single-blind, placebo-controlled, phase 1 trial. *Lancet* 2014; 383:60–8.
- Sorensen B, Mant T, Georgiev P, Rangarajan S, Pasi KJ, Creagh D, et al. A Subcutaneously Administered Investigational RNAi Therapeutic (ALN-AT3) Targeting Antithrombin for Treatment of Hemophilia: Phase 1 Study Results in Subjects with Hemophilia A or B. International Society of Thrombosis and Hemostasis, Toronto, Canada. 2015. [updated 2015 Jun 23; cited 2015 Aug 23]. Available from: <http://www.alnylam.com/capella/presentations/aln-at3-isth-june2015/>.

6. Petrocca F, Lieberman J. Promise and challenge of RNA interference-based therapy for cancer. *J Clin Oncol* 2011;29:747-54.
7. Foulkes WD, Smith IE, Reis-Filho JS. Triple-negative breast cancer. *N Engl J Med* 2010;363:1938-48.
8. Lehmann BD, Bauer JA, Chen X, Sanders ME, Chakravarthy AB, Shyr Y, et al. Identification of human triple-negative breast cancer subtypes and pre-clinical models for selection of targeted therapies. *J Clin Invest* 2011;121:2750-67.
9. Metzger-Filho O, Tutt A, de Azambuja E, Saini KS, Viale G, Loi S, et al. Dissecting the heterogeneity of triple-negative breast cancer. *J Clin Oncol* 2012;30:1879-87.
10. McNamara JO II, Andrechek ER, Wang Y, Viles KD, Rempel RE, Gilboa E, et al. Cell type-specific delivery of siRNAs with aptamer-siRNA chimeras. *Nat Biotechnol* 2006;24:1005-15.
11. Dassie JP, Liu XY, Thomas GS, Whitaker RM, Thiel KW, Stockdale KR, et al. Systemic administration of optimized aptamer-siRNA chimeras promotes regression of PSMA-expressing tumors. *Nat Biotechnol* 2009;27:839-49.
12. Zhou J, Li H, Li S, Zaia J, Rossi JJ. Novel dual inhibitory function aptamer-siRNA delivery system for HIV-1 therapy. *Mol Ther* 2008;16:1481-9.
13. Neff CP, Zhou J, Remling L, Kuruvilla J, Zhang J, Li H, et al. An aptamer-siRNA chimera suppresses HIV-1 viral loads and protects from helper CD4 (+) T cell decline in humanized mice. *Sci Transl Med* 2011;3:66ra66.
14. Kim MY, Jeong S. In vitro selection of RNA aptamer and specific targeting of ErbB2 in breast cancer cells. *Nucleic Acid Ther* 2011;21:173-8.
15. Wheeler LA, Trifonova R, Vrbanac V, Basar E, McKernan S, Xu Z, et al. Inhibition of HIV transmission in human cervicovaginal explants and humanized mice using CD4 aptamer-siRNA chimeras. *J Clin Invest* 2011;121:2401-12.
16. Thiel KW, Hernandez LI, Dassie JP, Thiel WH, Liu X, Stockdale KR, et al. Delivery of chemo-sensitizing siRNAs to HER2+ breast cancer cells using RNA aptamers. *Nucleic Acids Res* 2012;40:6319-37.
17. Pastor F, Kolonias D, Giangrande PH, Gilboa E. Induction of tumour immunity by targeted inhibition of nonsense-mediated mRNA decay. *Nature* 2010;465:227-30.
18. Wheeler LA, Vrbanac V, Trifonova R, Brehm MA, Gilboa-Geffen A, Tanno S, et al. Durable knockdown and protection from HIV transmission in humanized mice treated with gel-formulated CD4 aptamer-siRNA chimeras. *Mol Ther* 2013;21:1378-89.
19. Shigdar S, Lin J, Yu Y, Pastuovic M, Wei M, Duan W. RNA aptamer against a cancer stem cell marker epithelial cell adhesion molecule. *Cancer Sci* 2011;102:991-8.
20. Stingl J, Eaves CJ, Zandieh I, Emerman JT. Characterization of bipotent mammary epithelial progenitor cells in normal adult human breast tissue. *Breast Cancer Res Treat* 2001;67:93-109.
21. Osta WA, Chen Y, Mikhitarian K, Mitas M, Salem M, Hannun YA, et al. EpCAM is overexpressed in breast cancer and is a potential target for breast cancer gene therapy. *Cancer Res* 2004;64:5818-24.
22. Marhaba R, Klingbeil P, Nuebel T, Nazarenko I, Buechler MW, Zoeller M. CD44 and EpCAM: cancer-initiating cell markers. *Curr Mol Med* 2008;8:784-804.
23. Spizzo G, Fong D, Wurm M, Ensinger C, Obrist P, Hofer C, et al. EpCAM expression in primary tumour tissues and metastases: an immunohistochemical analysis. *J Clin Pathol* 2011;64:415-20.
24. Sarrjo D, Franklin CK, Mackay A, Reis-Filho JS, Isacke CM. Epithelial and mesenchymal subpopulations within normal basal breast cell lines exhibit distinct stem cell/progenitor properties. *Stem Cells* 2012;30:292-303.
25. Soysal SD, Muenst S, Barbie T, Fleming T, Gao F, Spizzo G, et al. EpCAM expression varies significantly and is differentially associated with prognosis in the luminal B HER2(+), basal-like, and HER2 intrinsic subtypes of breast cancer. *Br J Cancer* 2013;108:1480-7.
26. Imrich S, Hachmeister M, Gires O. EpCAM and its potential role in tumor-initiating cells. *Cell Adh Migr* 2012;6:30-8.
27. Munz M, Baeuerle PA, Gires O. The emerging role of EpCAM in cancer and stem cell signaling. *Cancer Res* 2009;69:5627-9.
28. Federici G, Espina V, Liotta L, Edmiston KH. Breast cancer stem cells: a new target for therapy. *Oncology* 2011;25:25-8, 30.
29. Ladwein M, Pape UF, Schmidt DS, Schnolzer M, Fiedler S, Langbein L, et al. The cell-cell adhesion molecule EpCAM interacts directly with the tight junction protein claudin-7. *Exp Cell Res* 2005;309:345-57.
30. Gonzalez B, Denzel S, Mack B, Conrad M, Gires O. EpCAM is involved in maintenance of the murine embryonic stem cell phenotype. *Stem Cells* 2009;27:1782-91.
31. Lu TY, Lu RM, Liao MY, Yu J, Chung CH, Kao CF, et al. Epithelial cell adhesion molecule regulation is associated with the maintenance of the undifferentiated phenotype of human embryonic stem cells. *J Biol Chem* 2010;285:8719-32.
32. Schulze K, Gasch C, Staufer K, Nashan B, Lohse AW, Pantel K, et al. Presence of EpCAM-positive circulating tumor cells as biomarker for systemic disease strongly correlates to survival in patients with hepatocellular carcinoma. *Int J Cancer* 2013;133:2165-71.
33. Konigsberg R, Obermayr E, Bises G, Pfeiler G, Gneist M, Wrba F, et al. Detection of EpCAM positive and negative circulating tumor cells in metastatic breast cancer patients. *Acta Oncol* 2011;50:700-10.
34. Weissenstein U, Schumann A, Reif M, Link S, Toffol-Schmidt UD, Heusser P. Detection of circulating tumor cells in blood of metastatic breast cancer patients using a combination of cytokeratin and EpCAM antibodies. *BMC Cancer* 2012;12:206.
35. Zhao S, Yang H, Zhang M, Zhang D, Liu Y, Song Y, et al. Circulating tumor cells (CTCs) detected by triple-marker EpCAM, CK19, and hMAM RT-PCR and their relation to clinical outcome in metastatic breast cancer patients. *Cell Biochem Biophys* 2013;65:263-73.
36. Chen Q, Ge F, Cui W, Wang F, Yang Z, Guo Y, et al. Lung cancer circulating tumor cells isolated by the EpCAM-independent enrichment strategy correlate with Cytokeratin 19-derived CYFRA21-1 and pathological staging. *Clin Chim Acta* 2013;419:57-61.
37. Schmidt M, Scheulen ME, Dittrich C, Obrist P, Marschner N, Dirix L, et al. An open-label, randomized phase II study of adecatumumab, a fully human anti-EpCAM antibody, as monotherapy in patients with metastatic breast cancer. *Ann Oncol* 2010;21:275-82.
38. Marschner N, Ruttinger D, Zugmaier G, Nemere G, Lehmann J, Obrist P, et al. Phase II study of the human anti-epithelial cell adhesion molecule antibody adecatumumab in prostate cancer patients with increasing serum levels of prostate-specific antigen after radical prostatectomy. *Urol Int* 2010;85:386-95.
39. Schmidt M, Ruttinger D, Sebastian M, Hanusch CA, Marschner N, Baeuerle PA, et al. Phase IB study of the EpCAM antibody adecatumumab combined with docetaxel in patients with EpCAM-positive relapsed or refractory advanced-stage breast cancer. *Ann Oncol* 2012;23:2306-13.
40. Barretina J, Caponigro G, Stransky N, Venkatesan K, Margolin AA, Kim S, et al. The Cancer Cell Line Encyclopedia enables predictive modelling of anticancer drug sensitivity. *Nature* 2012;483:603-7.
41. Ince TA, Richardson AL, Bell GW, Saitoh M, Godar S, Karnoub AE, et al. Transformation of different human breast epithelial cell types leads to distinct tumor phenotypes. *Cancer Cell* 2007;12:160-70.
42. Daniels DA, Chen H, Hicke BJ, Swiderek KM, Gold L. A tenascin-C aptamer identified by tumor cell SELEX: systematic evolution of ligands by exponential enrichment. *Proc Natl Acad Sci U S A* 2003;100:15416-21.
43. Huang Z, Szostak JW. Evolution of aptamers with a new specificity and new secondary structures from an ATP aptamer. *RNA* 2003;9:1456-63.
44. Gold L, Janjic N, Jarvis T, Schneider D, Walker JJ, Wilcox SK, et al. Aptamers and the RNA world, past and present. *Cold Spring Harb Perspect Biol* 2012;4:a003582.
45. Zimmermann B, Gesell T, Chen D, Lorenz C, Schroeder R. Monitoring genomic sequences during SELEX using high-throughput sequencing: neutral SELEX. *PLoS ONE* 2010;5:e9169.
46. Burnett JC, Rossi JJ. RNA-based therapeutics: current progress and future prospects. *Chem Biol* 2012;19:60-71.
47. Dassie JP, Giangrande PH. Current progress on aptamer-targeted oligonucleotide therapeutics. *Ther Deliv* 2013;4:1527-46.
48. Keefe AD, Pai S, Ellington A. Aptamers as therapeutics. *Nat Rev Drug Discov* 2010;9:537-50.
49. Sundaram P, Kurniawan H, Byrne ME, Wower J. Therapeutic RNA aptamers in clinical trials. *Eur J Pharm Sci* 2013;48:259-71.
50. Kotula JW, Pratico ED, Ming X, Nakagawa O, Juliano RL, Sullenger BA. Aptamer-mediated delivery of splice-switching oligonucleotides to the nuclei of cancer cells. *Nucleic Acid Ther* 2012;22:187-95.
51. Esposito CL, Cerchia L, Catuogno S, De Vita G, Dassie JP, Santamaria G, et al. Multifunctional aptamer-miRNA conjugates for targeted cancer therapy. *Mol Ther* 2014;22:1151-63.



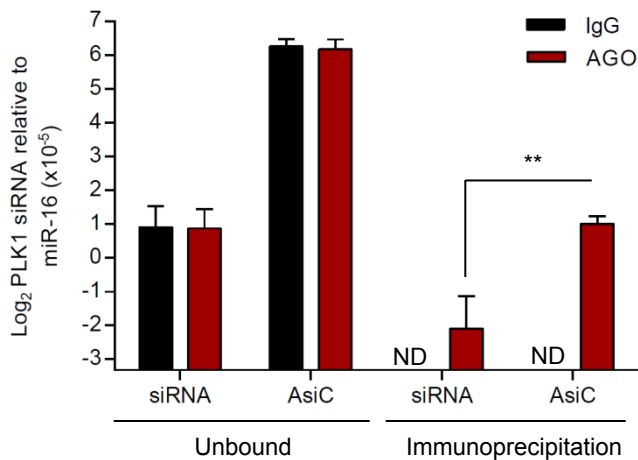
Supplemental Figure 1 – EpCAM-AsiCs are stable in human and mouse serum

eGFP EpCAM-AsiCs, synthesized using 2'-fluoro-pyrimidines, chemically stabilized cholesterol-conjugated *eGFP* siRNAs (chol-siRNA), or unmodified *eGFP* siRNAs were incubated at 37°C in 50% human or mouse serum. Aliquots were removed at regular intervals and stored at -80°C before electrophoresis on denaturing PAGE gels. The average intensity (+S.E.M.) of bands from 2 independent experiments quantified by densitometry after ethidium bromide staining is shown.

a**b**

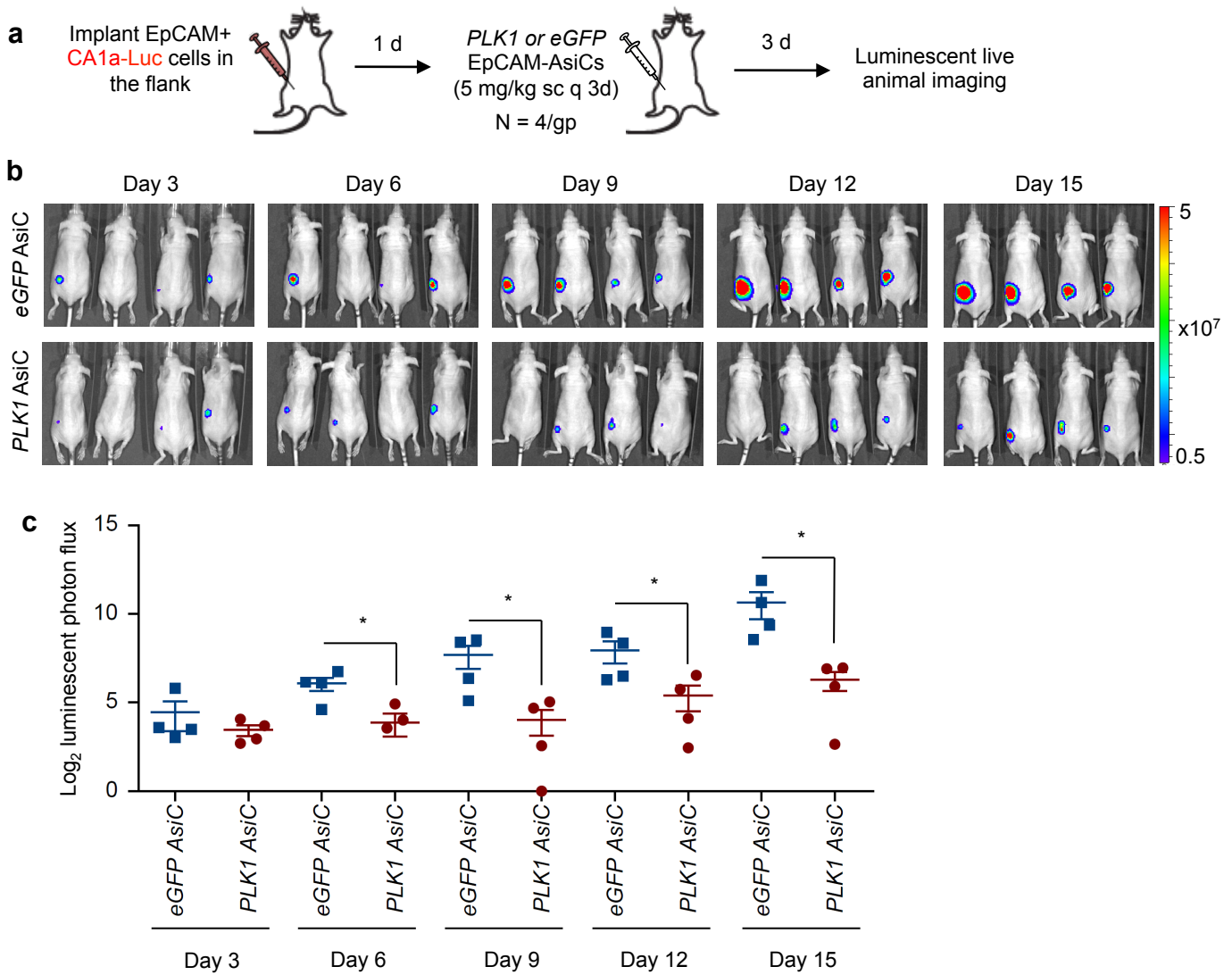
Supplemental Figure 2 - Injection of EpCAM-AsiCs does not stimulate innate immunity

Mice were injected sc with eGFP EpCAM-AsiCs (5 mg/kg, n=3) or ip with Poly(I:C) (5 or 50 mg/kg (n=2/dose)). **a**, Serum samples, collected at baseline and 6 and 16 hr after treatment were assessed for IFN β , IL-6 and IP-10 by multiplex immunoassay. *, $P < 0.05$; **, $P < 0.01$; ***, $P < 0.001$; compared to baseline. **b**, mRNA expression of cytokine and IFN-induced genes, relative to *Gapdh* was assayed by qRT-PCR in total splenocytes harvested 16 hr post treatment. **, $P < 0.01$, compared to untreated (NT, n=3).



Supplemental Figure 3 – *PLK1* siRNA associates with Argonaute (AGO) in cells treated with *PLK1* EpCAM-AsiCs

MB-468 cells, treated with *PLK1* EPCAM-AsiC or siRNA for 2 days, were lysed, and cell lysates were immunoprecipitated with pan-AGO antibody or IgG isotype control. The amount of *PLK1* siRNA in the immunoprecipitates was quantified by Taqman qRT-PCR, presented as \log_2 mean with SEM, relative to miR-16. **, $P < 0.01$ by Student's t-test relative to siRNA-treated cells. ND, not detectable. *PLK1* siRNA was found in the RISC after treatment with *PLK1* EpCAM-AsiCs. However, the Ago immunoprecipitation did not significantly deplete *PLK1* siRNAs from the supernatant. This is likely because most RNAs that are taken up by cells are not released from endosomes to the cytosol (A. Wittrup et al., Visualizing lipid-formulated siRNA release from endosomes and target gene knockdown. Nature Biotechnology 2015, in press).



Supplemental Figure 4 - PLK EpCAM AsiC suppresses MCF10CA1a (CA1a) tumor growth.

a, Experimental scheme. In this experiment the AsiCs were injected sc in the flank near the tumor, but not into the tumor. **b**, Bioluminescent images of treated mice. Heat map indicates photon flux (photon/second/cm²). **c**, Log₂ total luminescent photon flux of the tumors (N = 4); *, P < 0.05 by Student's t-test.

Supplemental Table 1. EpCAM-AsiC Sequences

AsiC construct	Sequence
EpCAM PLK1 sense	GCG ACU GGU UAC CCG GUC GUU UUG AAG AAG AUC ACC CUC CUU AdTdT
EpCAM PLK1 anti-sense	UAA GGA GGG UGA UCU UCU UCA dTdT
EpCAM AKT1 sense	GCG ACU GGU UAC CCG GUC GUU GCU GGA GAA CCU CAU GCU GdTdT
EpCAM AKT1 anti-sense	CAG CAU GAG GUU CUC CAG CdTdT
EpCAM GFP sense	GCG ACU GGU UAC CCG GUC GUU UGG CUA CGU CCA GGA GCG CAdTdT
EpCAM GFP anti-sense	UGC GCU CCU GGA CGU AGC CdTdT
siGFP sense	UGG CUA CGU CCA GGA GCG
siGFP antisense	UGC GCU CCU GGA CGU AGC
siAKT1 sense	GCU GGA GAA CCU CAU GCU G
siAKT1 antisense	CAG CAU GAG GUU CUC CAG C
siPLK1 sense	UGA AGA AGA UCA CCC UCC UUA
siPLK1 antisense	UAA GGA GGG UGA UCU UCU UCA